

Communication

Preparation of Few-Layer Graphene Dispersions from Hydrothermally Expanded Graphite

Cristian Vacacela Gomez ^{1,2,*} , Talia Tene ¹, Marco Guevara ^{1,3}, Gabriela Tubon Usca ^{1,4},
Dennys Colcha ¹, Hannibal Brito ⁵, Raul Molina ², Stefano Bellucci ⁶ and Adalgisa Tavolaro ⁴ 

¹ Physics Research Group, Faculty of Science, Escuela Superior Politécnica de Chimborazo, Riobamba EC060101, Ecuador; talia.tene@esPOCH.edu.ec (T.T.); marco.guevara@esPOCH.edu.ec (M.G.); gabytubon@gmail.com (G.T.U.); dcolcha1@gmail.com (D.C.)

² GraphenTech NL, Olympiaweg 28A, 3077AL Rotterdam, The Netherlands; rm@redecua.com

³ Faculty of Mechanical Engineering, Escuela Superior Politécnica de Chimborazo, Riobamba EC060101, Ecuador

⁴ Research Institute on Membrane Technology (ITM - CNR), Cubo 17C, 87036 University of Calabria, 87036 Cosenza, Italy; a.tavolaro@itm.cnr.it

⁵ Grupo de Investigación en Ambiente y Desarrollo, Escuela Superior Politécnica de Chimborazo, Riobamba EC060101, Ecuador; hannibal.brito@esPOCH.edu.ec

⁶ INFN-Laboratori Nazionali di Frascati, Via E. Fermi 40, I-00044 Frascati, Italy; Stefano.Bellucci@lnf.infn.it

* Correspondence: cristian.vacacelag@esPOCH.edu.ec

Received: 28 May 2019; Accepted: 18 June 2019; Published: 21 June 2019



Abstract: In this study, we propose a novel approach to prepare few-layer graphene (FLG) dispersions, which is realized by exfoliating natural graphite flakes in a surfactant aqueous solution under hydrothermal treatment and liquid-phase exfoliation. In order to obtain stable and well-dispersed FLG dispersions, pristine graphite is hydrothermally expanded in a hexadecyltrimethylammonium bromide (CTAB) aqueous solution at 180 °C for 15 h, followed by sonication up to 3 h. In comparison to long-time sonication methods, the present method is significantly efficient, and most importantly, does not involve the use of an oxidizing agent and hazardous media, which will make it more competent in the scalable production of graphene.

Keywords: few-layer graphene; CTAB; hydrothermal treatment; sonication

1. Introduction

Owing to its outstanding physical and chemical properties [1,2], graphene has become the most studied nanomaterial of the past decade. Until now, many top-down methods have developed for preparing graphene, such as micromechanical cleavage of graphite [3], oxidation-reduction of graphite [4,5], electrochemical exfoliation of graphite [6], and liquid-phase exfoliation of graphite [7]. Among them, the liquid-phase exfoliation is the most commonly used method to prepare graphene by sonication at a low cost and with minimal environmental impact. However, this method mostly involves the use of high-boiling point solvents, e.g., N-methyl-pyrrolidone (NMP) [8] and a long sonication time to reach high concentrations of dispersed graphene [9].

A viable liquid-phase exfoliation route is carried out in an aqueous solution through suitable surfactants [10] (and biosurfactants [11]) that reduce and optimize the high surface energy of water to match with highly hydrophobic graphitic surfaces [12]. Surfactants offer the steric and electrostatic repulsion that is necessary to avoid the graphene sheets from aggregation due to the sonication which breaks up graphite into few-layer graphene (FLG) flakes that are coated by the surfactant molecules [12,13]. Surfactants, therefore, are excellent candidates in the direct exfoliation of graphite because they are used as a dispersant and a stabilizer.

In an effort to circumvent long sonication time limitations (e.g., the induced defects in graphene structure [14]), Ou et al. [15] successfully demonstrated the preparation of FLG dispersions from graphite powder, in a relatively short sonication time by combining heat-treatment in NMP and liquid-phase exfoliation in different organic solvents. The heat-treatment increases the interlayer distance of graphite, which is stabilized by adding polyvinyl pyrrolidone (PVP), followed by sonication for up to 20 h to prepare well-dispersed FLG dispersions. To our knowledge, an alternative method that combines heat-treatment of natural graphite flakes and direct exfoliation in stabilizing surfactants is unexplored, particularly, at a short sonication time.

In this study, we propose such a method to prepare FLG dispersions in surfactant water solution using hydrothermal treatment and liquid-phase exfoliation. First, we subject pristine natural graphite to temperature to produce pretreated graphite flakes. Subsequently, pretreated graphite is exfoliated into FLG by sonication and centrifugation. The cationic surfactant, hexadecyltrimethylammonium bromide (CTAB), is selected as a dispersant and a stabilizer [16,17]. CTAB is commonly considered as the dispersing agent to stabilize aqueous solutions of graphene [18] and it has also been used as the precursor for preparing graphene nanocomposites [19] with promising applications in electrochemical sensing and biosensing [20].

2. Materials and Methods

Natural graphite flakes were purchased from Pingdu Huadong Graphite Co. Ltd., and the CTAB (H5882-100G, 98%, M.W. 364.45) was purchased from Sigma Aldrich. The graphite and the CTAB were used as received, without further purification. In a typical experiment, 100 mg of natural graphite flakes were added into 50 mL of CTAB aqueous solution at different surfactant concentrations (i.e., 0.1, 0.5, and 1.0 mg mL⁻¹). The resulting mixture was transferred into a sealed Teflon vessel (100 mL) and reacted at 180 °C for 15 h (optimal parameters reported in [15,21]) to obtain pretreated graphite. After the hydrothermal treatment (HT), pretreated graphite was immediately dispersed in the very same CTAB aqueous solution by sonication, employing a tip sonicator (UP100H-Hielscher, 50 watts, 30 kHz) in continuous operation. To reduce the damage to the graphene sheets by ultrasonic processing, the maximum sonication time was 3 h. The sonication produced black suspensions that were left to stand overnight and then centrifugated for 90 min at 2000 rpm (optimal parameters reported in [22]) to remove nonexfoliated graphite flakes. After centrifugation, the pipette-extracted 40 mL supernatant was semitransparent without the presence of agglomerates (Supplementary Figure S1). The concentration of dispersed graphene was determined by UV-visible absorption spectroscopy and the absorbance (*A*) was adapted to calculate the concentration using the Beer–Lambert law (a widely used approach [10,22,23]):

$$C_G = \frac{A}{l \cdot \alpha_{660}}$$

where, *l* = 0.01 m, is the path length and $\alpha = 1390 \text{ mL mg}^{-1} \text{ m}^{-1}$, is the absorption coefficient of the dispersed graphene in the surfactant water solutions [10]. The characteristic absorption spectra of the dispersed graphene were recorded using UV-vis spectroscopy (UV-160A, Shimadzu Corporation, Japan). The morphologies of the samples were observed using a scanning electron microscopy (SEM, Quanta Feg 400 F7) with accelerating voltage ranging from 5 to 35 kV. Raman spectra were obtained using a Jobin Yvon LABRAM spectrometer, with a 514 nm laser wavelength.

3. Results and Discussions

To begin, we briefly analyze the hydrothermal conditions, the sonication process, the surfactant effect, and the yield. Supplementary Figure S2 shows the schematic route of the preparation process for graphene dispersions. Under hydrothermal conditions, various factors affect the graphite crystal structure which include temperature and pressure. Temperature generates water vapor, and pressure origins changes in the kinetics of reactions affecting the graphite structure [24]. Therefore, temperature and pressure create conditions for the intercalation of the CTAB (and water) molecules between

graphene layers [25]. The intercalation increases the interlayer distance of graphite which is crucial to the improvement of the subsequent ultrasonication process [15].

Ultrasonication is described by the effect of acoustic cavitation of high frequency ultrasound in the formation, growth, and collapse of microbubbles in solution, which induces shock waves on the graphite surface, producing exfoliation of graphite into FLG [26]. Notwithstanding, the direct exfoliation of graphite in water is possible and the resulting exfoliated graphene flakes are not stable. The CTAB molecules have a cationic ammonium head group and an extended alkyl chain as a tail [26]. It is expected that the CTAB molecules are adsorbed onto the graphene surface through electrostatic interactions [25]. The hydrophobic interaction of the alkyl chains of the CTAB molecules on the graphene surface prevents the re-stacking and agglomeration of exfoliated flakes.

The yield of this approach, based on the absorption coefficient of [10], was ~5% and needs to be optimized. At this point, the apparent low concentration of dispersed graphene in comparison with the relative amount of CTAB, is the result of using the absorbance to calculate the concentration by the Beer–Lambert law. Since this approach is usually used to obtain the concentration of dispersed graphene [10,22,23], it is employed to emphasize the role of hydrothermal treatment instead of its final yield. Attempts to improve the yield are currently in progress using the gravimetric method and extending the study for cationic/anionic surfactants.

Pristine (gray) graphite and pretreated (light-yellow) graphite are shown in Figure 1a,b, respectively. The optical change is due to the interaction of graphite with the surfactant, and therefore the obtained light-yellow graphite is due to the presence of molecular bromine because the resulting pretreated graphite was not washed after HT, which is verified by the surfactant bubbles in Figure 1b. Since pretreated graphite is dispersed in the very same CTAB aqueous solution, sonication is immediately used to simplify the method.

In order to understand the role of HT, Figure 1a,b present the concentration of dispersed graphene considering different amounts of CTAB and different sonication times. Again, we stress that this study is limited to 3 h of sonication, however it is well-known that the exfoliation yield is increased by increasing the sonication time, and a suitable sonication time is 10 h [15]. We show, however, that the concentration of dispersed graphene from pretreated graphite is significantly enhanced, suggesting that HT plays a crucial role. Therefore, depending on the amount of CTAB, sonication time, and HT, the concentration of dispersed graphene ranges from 40 $\mu\text{g mL}^{-1}$ to 60 $\mu\text{g mL}^{-1}$. These concentrations are comparable to those obtained in early studies by exfoliating graphite with a long sonication time [22,27].

CTAB seems to be an efficient dispersant at high concentrations (0.5, 1.0 mg mL^{-1}). However, high quantities of surfactant may have a significant impact on the electrical properties of graphene because the residual surfactant is difficult to remove [28]. To circumvent this, we focus on graphene dispersions obtained at the lowest concentration of CTAB (0.1 mg mL^{-1}) and after 3 h of sonication. Figure 1c shows the stability of graphene dispersions, at the lowest concentration of CTAB, obtained from pretreated and pristine graphite. In both cases, graphene flakes are easy to precipitate, as the storage time increases, however, it is noteworthy that the stability of graphene dispersion obtained from pretreated graphite is higher than from pristine graphite within 12 weeks. These results corroborate the importance of HT. The UV-visible absorption spectra of graphene dispersions, after 3 h of sonication and different CTAB concentrations, are shown in Figure 1d. The spectra are featureless in the visible region as expected for graphene. A prominent peak is found at ~266 nm, corresponding to the π to π^* transitions of graphene and graphite [29].

Previously, the transformation of the graphite (powder) structure, after heat-treatment in NMP, was effectively demonstrated by SEM, Raman, and X-ray diffraction (XRD) measurements, i.e., the increased interlayer spacing of graphite as a direct consequence of increasing the heat [15]. In Figure 2, we confirm this fact by scrutinizing the morphology of pretreated (natural) graphite flakes considering the different amounts of CTAB.

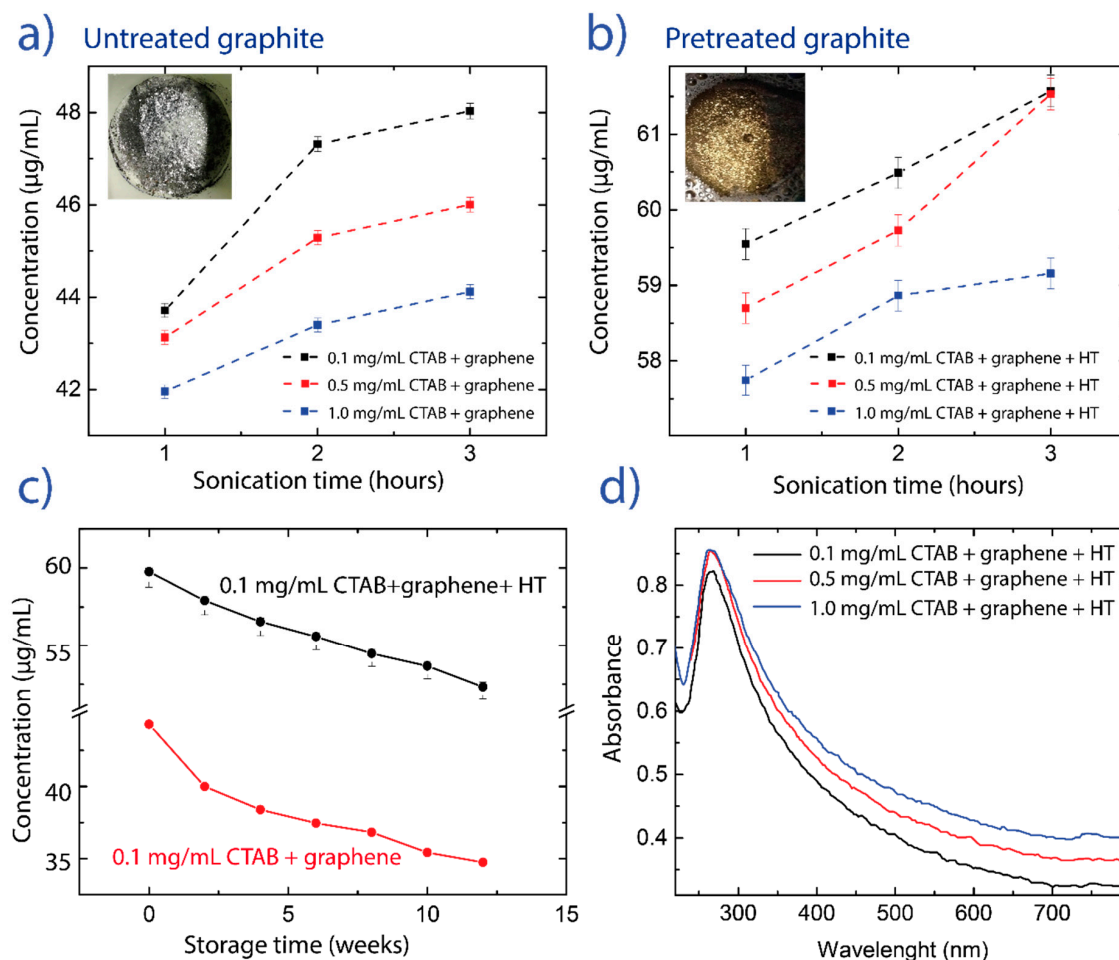


Figure 1. Concentration of dispersed graphene as a function of three different hexadecyltrimethylammonium bromide (CTAB) concentrations (0.1, 0.5, 1.0 mg/mL^{-1}) at three different sonication times, from (a) pristine (untreated) graphite and (b) treated graphite by the hydrothermal treatment (HT). (c) Stability of the graphene dispersion in 0.1 mg/mL^{-1} of the CTAB aqueous solution as a function of the storage time, considering pristine and pretreated graphite source. (d) UV-visible spectra of exfoliated graphene in the three different CTAB concentrations after HT and 3 h of sonication. Optical photos of pristine graphite (a, inset) and pretreated graphite (b, inset).

Independently of the CTAB concentration (0.1, 0.5 and 1.0 mg mL^{-1}), as shown in Figure 2a–c, HT also increases the interlayer spacing of graphite which is stabilized by surfactant. Therefore, the resulting pretreated graphite is called hydrothermally expanded graphite (HEG). At the highest concentration of CTAB, in Figure 2a, we show the surfactant intercalation (green arrows) and the HEG surface coated by the surfactant molecules (green dashed circle). After 3 h of sonication in the three different CTAB concentrations, Figure 2d–f demonstrate that graphene dispersions are composed of smaller and thinner layers.

These layers seem to be semitransparent and surfactant-free, which is interpreted as an important result for future applications in electronic devices. However, by scrutinizing the morphology of layers at the highest concentration of CTAB and by changing the accelerating voltage from 5 to 30 kV, in Supplementary Figure S3, we observe the presence of surfactant which corroborates the statement about the difficulty of the residual surfactant removal and the need to use the proposed method at the lowest concentration of CTAB in order to prevent the intrinsic properties of the obtained layers.

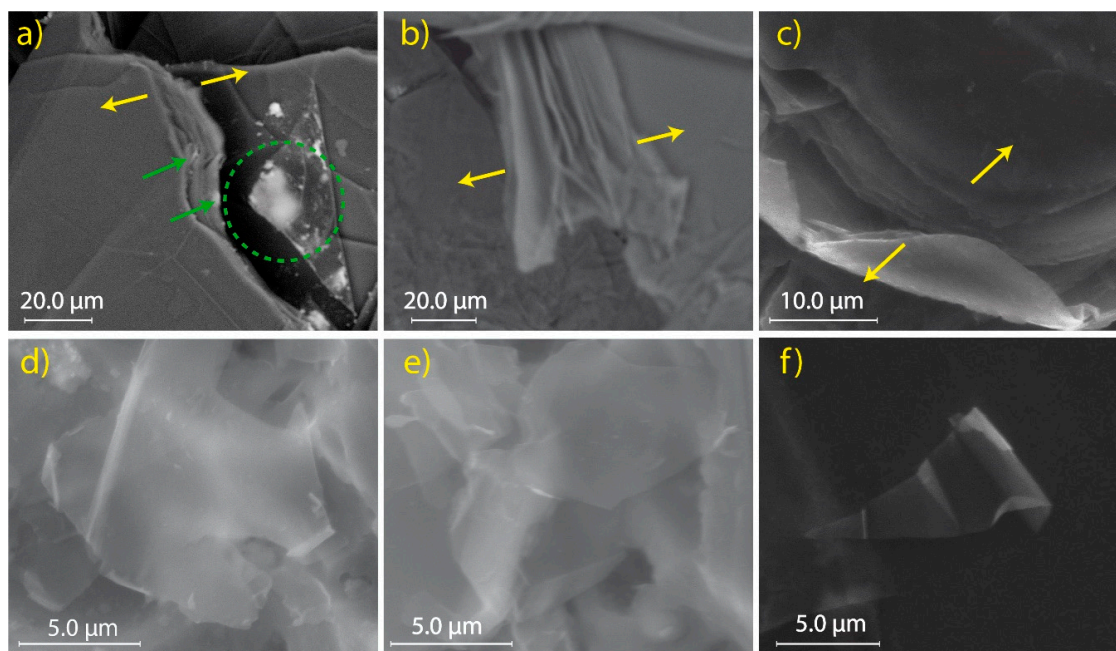


Figure 2. Scanning electron microscopy (SEM) morphology of pretreated natural graphite in (a) 1.0 mg mL⁻¹, (b) 0.5 mg mL⁻¹, and (c) 0.1 mg mL⁻¹ of CTAB aqueous solution. (d–f) Semitransparent layers obtained from supernatant after 2000 rpm centrifugation for 90 min, subject to 3 h of sonication in the three different CTAB concentrations.

The Raman spectrum of graphite and dispersed graphene (at the lowest concentration of CTAB, after HT and 3 h of sonication) are reported in Figure 3. We detect the three major peaks, i.e., the D peak at ~ 1340 cm⁻¹, the G peak at ~ 1580 cm⁻¹ (~ 572 cm⁻¹), and the 2D peak at ~ 2719 cm⁻¹ (~ 2711 cm⁻¹). The D peak and G peak are attributed to the edge/basal defects and the ordered sp^2 -hybridized carbon bonds in the graphene/graphite lattice, respectively. In dispersed graphene, the peak ratio between the intensity of D and G peaks (I_D/I_G) is 0.28, indicating that some edge/basal defects are induced during the process of ultrasonication [30]. Probably, the small size and folded edge of graphene layers (Figure 2d–f), contributes significantly to the observed D peak, although we cannot completely rule out the presence of in-plane defects.

The structure of G peak observed in the dispersed graphene at ~ 1572 cm⁻¹ appears to be slightly affected by the presence of D' peak, however, the D' peak usually is present when there are surface defects, such as charging or other impurities adsorbed onto the surface [31]. The latter here is attributed to the remaining surfactant as observed in Supplementary Figure S3 at the highest concentration of CTAB, which strongly confirms the need to use our method at low concentrations of surfactant. Interestingly enough, the D and G (G and D') peaks of our graphene sample are well separated from each other and are distinctly different from those of graphene oxide, in which case the D and G peaks are broad and overlap. This fact suggests that our dispersed graphene did not undergo severe in-plane disruption as in the case of graphene oxide [30].

The peak is slightly broader between 2625 and 2700 cm⁻¹ and it is commonly used to estimate the number of layers in obtained graphene [32]. However, the intensity of the 2D peak depends on the excitation laser frequency, and therefore cannot be solely relied upon [31]. In this context, we use the full width at half maximum (FWHM) to evaluate the 2D peak, which is found to be a qualitative guide to distinguish the number of layers from single- to five-layer graphene [33]. By fitting the 2D peak with two Lorentzian functions, the intensity of the 2D_{1A} peak (detected at ~ 2683 cm⁻¹) increases in dispersed graphene, with respect to the intensity of the 2D_{1A} peak (at ~ 2676 cm⁻¹) in pristine graphite. Most importantly, in Supplementary Figures S4 and S5, we report the FWHM of 2D_{1A} = 68.3 ± 1.6 cm⁻¹, 2D_{2A} = 36.9 ± 1.0 cm⁻¹, and 2D = 68.7 ± 1.1 cm⁻¹, respectively. These values are in good agreement

with previous reports for tri-, four-, and five-layer graphene [33]. Furthermore, the 2D peak became more symmetrical in dispersed graphene, after HT and sonication, indicating the presence of FLG in obtained graphene dispersions.

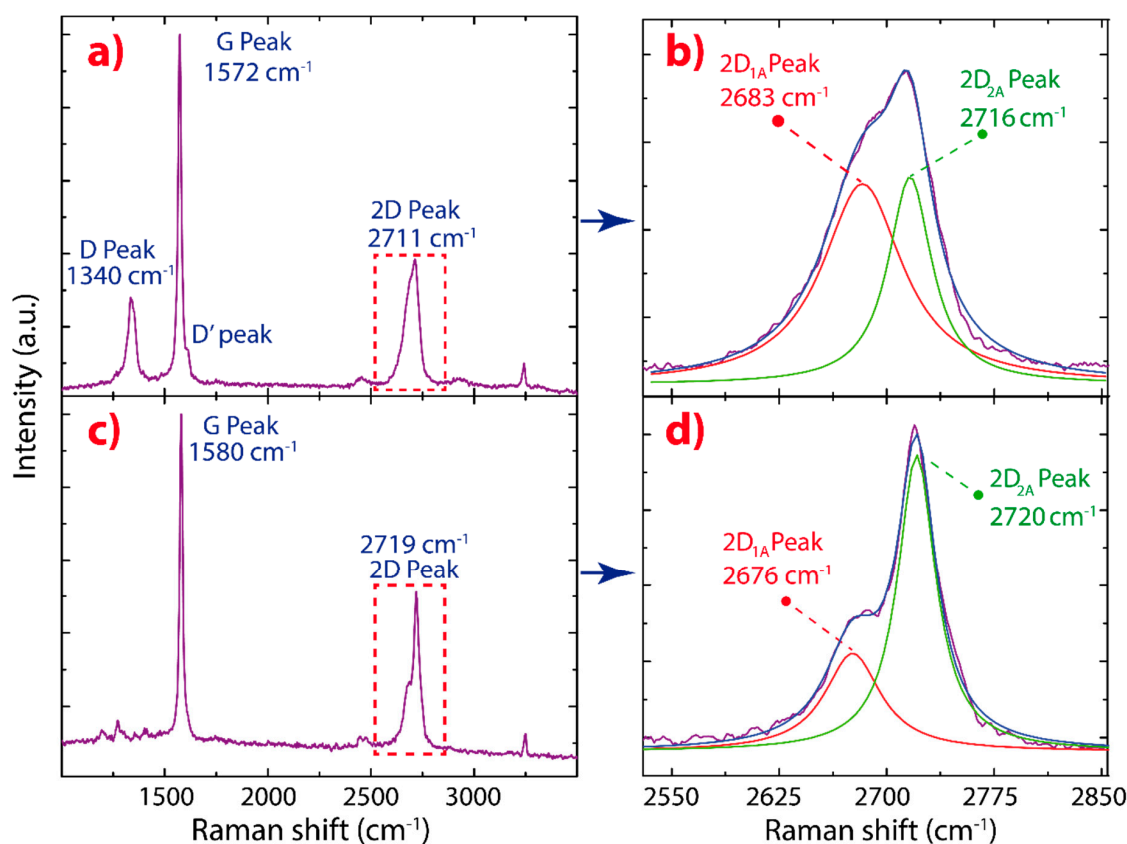


Figure 3. Raman spectra of (a) dispersed graphene after hydrothermal treatment and 3 h of sonication in 0.1 mg mL^{-1} CTAB aqueous solution, fabricated by drop casting of dispersion, and (c) pristine graphite. (b–d) Fitting of the 2D peaks with two Lorentzian functions. The intensity was normalized by the G peak.

4. Conclusions

In this study, a simple method to prepare graphene dispersions has been demonstrated. Natural graphite flakes were effectively exfoliated into FLG under HT and liquid-phase exfoliation in a surfactant aqueous solution. The cationic surfactant, CTAB, was used as a dispersant and a stabilizer. First, pristine graphite was hydrothermally expanded in the CTAB aqueous solution reacted at $180 \text{ }^\circ\text{C}$ for 15 h. Subsequently, pretreated graphite (denominated as hydrothermally expanded graphite, HEG) was exfoliated into FLG by sonication for 3 h, producing stable and well-dispersed graphene dispersions. The expansion of interlayer spacing of graphite was demonstrated using SEM measurements. The efficiency of HT was estimated by measuring the concentration of the dispersed graphene which was shown to be comparable to graphene dispersions reported with a long sonication time [22,27]. Depending on the amount of the CTAB, sonication time, and HT, the concentration of dispersed graphene ranged from $40 \text{ } \mu\text{g mL}^{-1}$ to $60 \text{ } \mu\text{g mL}^{-1}$. The obtained graphene dispersions from pretreated graphite were shown to have good stability within 12 weeks. Using Raman analyses, the obtained FLG presented lower (edge/basal) defects, and most importantly, based on the FWHM analysis, we confirmed the presence of FLG, likely, no more than five layers. This novel approach (but non-optimized) may be explored in the future for cationic/anionic surfactants (or biosurfactants) in order to improve its efficiency.

Supplementary Materials: The following are available online at <http://www.mdpi.com/2076-3417/9/12/2539/s1>, Figure S1: Obtained graphene dispersions (12 weeks stored) after hydrothermal treatment (HT), 3 h of sonication and centrifugation, in the three different concentrations of CTAB (0.1, 0.5, and 1.0 mg mL⁻¹) reported in the main text. After sonication, the obtained suspensions were left to stand overnight and then centrifugated for 90 min at 2000 rpm., Figure S2: Schematic route of the preparation process for FLG dispersions. Natural graphite flakes are added into CTAB aqueous solution (at different surfactant concentrations: 0.1, 0.5, and 1.0 mg mL⁻¹). The resulting mixture is reacted at 180 °C for 15 h. The obtained pretreated graphite is immediately dispersed in the very same CTAB aqueous solution by sonication, Figure S3: Scanning electron microscopy (SEM) morphology of dispersed graphene layer in 1.0 mg mL⁻¹ of CTAB aqueous solution, by changing the accelerating voltage from 5 to 30 kV. Semitransparent layer extracted from supernatant after HT, 3 h of sonication, centrifugation for 90 min at 2000 rpm, and dried at 235 °C, Figure S4: Raman spectrum of the 2D peak of dispersed graphene in 0.1 mg mL⁻¹ of CTAB aqueous solution and fitting of the 2D peaks with two Lorentzian functions. The w values represent the respective full width at half maximum (FWHM) values, Figure S5: Raman spectrum of the 2D peak of dispersed graphene in 0.1 mg mL⁻¹ of CTAB aqueous solution and fitting of the 2D peaks with one Lorentzian function. The w value represents the respective FWHM value.

Author Contributions: All authors contributed to designing and performing measurements, data analysis, scientific discussions, and writing the article.

Funding: This research received no external funding.

Acknowledgments: We acknowledge E. Cazzanelli for helping us with Raman measurements, as well as L. Caputi, Diana Coello-Fiallos, and Richard Pachacama for the stimulating discussions.

Conflicts of Interest: The authors declare no conflict of interest.

References

1. Coello-Fiallos, D.; Tene, T.; Guayllas, J.L.; Haro, D.; Haro, A.; Gomez, C.V. DFT comparison of structural and electronic properties of graphene and germanene: Monolayer and bilayer systems. *Mater. Today Proc.* **2017**, *4*, 6835–6841. [[CrossRef](#)]
2. Dreyer, D.R.; Park, S.; Bielawski, C.W.; Ruoff, R.S. The chemistry of graphene oxide. *Chem. Soc. Rev.* **2010**, *39*, 228–240. [[CrossRef](#)] [[PubMed](#)]
3. Yi, M.; Shen, Z. A review on mechanical exfoliation for the scalable production of graphene. *J. Mater. Chem. A* **2015**, *3*, 11700–11715. [[CrossRef](#)]
4. Chen, W.; Yan, L.; Bangal, P.R. Preparation of graphene by the rapid and mild thermal reduction of graphene oxide induced by microwaves. *Carbon* **2010**, *48*, 1146–1152. [[CrossRef](#)]
5. Gomez, C.V.; Robalino, E.; Haro, D.; Tene, T.; Escudero, P.; Haro, A.; Orbe, J. Structural and electronic properties of graphene oxide for different degree of oxidation. *Mater. Today Proc.* **2016**, *3*, 796–802. [[CrossRef](#)]
6. Parvez, K.; Li, R.; Puniredd, S.R.; Hernandez, Y.; Hinkel, F.; Wang, S.; Müllen, K. Electrochemically exfoliated graphene as solution-processable, highly conductive electrodes for organic electronics. *ACS Nano* **2013**, *7*, 3598–3606. [[CrossRef](#)] [[PubMed](#)]
7. Hernandez, Y.; Nicolosi, V.; Lotya, M.; Blighe, F.M.; Sun, Z.; De, S.; Boland, J.J. High-yield production of graphene by liquid-phase exfoliation of graphite. *Nat. Nanotechnol.* **2008**, *3*, 563. [[CrossRef](#)]
8. Usca, G.T.; Hernandez-Ambato, J.; Pace, C.; Caputi, L.S.; Tavolaro, A. Liquid-phase exfoliated graphene self-assembled films: Low-frequency noise and thermal-electric characterization. *Appl. Surf. Sci.* **2016**, *380*, 268–273. [[CrossRef](#)]
9. Khan, U.; O'Neill, A.; Lotya, M.; De, S.; Coleman, J.N. High-concentration solvent exfoliation of graphene. *Small* **2010**, *6*, 864–871. [[CrossRef](#)]
10. Lotya, M.; Hernandez, Y.; King, P.J.; Smith, R.J.; Nicolosi, V.; Karlsson, L.S.; Duesberg, G.S. Liquid phase production of graphene by exfoliation of graphite in surfactant/water solutions. *J. Am. Chem. Soc.* **2009**, *131*, 3611–3620. [[CrossRef](#)]
11. Ba, H.; Truong-Phuoc, L.; Pham-Huu, C.; Luo, W.; Baaziz, W.; Romero, T.; Janowska, I. Colloid Approach to the Sustainable Top-Down Synthesis of Layered Materials. *ACS Omega* **2017**, *2*, 8610–8617. [[CrossRef](#)]
12. Narayan, R.; Kim, S.O. Surfactant mediated liquid phase exfoliation of graphene. *Nano Converg.* **2015**, *2*, 20. [[CrossRef](#)] [[PubMed](#)]
13. Smith, R.J.; Lotya, M.; Coleman, J.N. The importance of repulsive potential barriers for the dispersion of graphene using surfactants. *New J. Phys.* **2010**, *12*, 125008. [[CrossRef](#)]

14. Ciesielski, A.; Samori, P. Graphene via sonication assisted liquid-phase exfoliation. *Chem. Soc. Rev.* **2014**, *43*, 381–398. [[CrossRef](#)] [[PubMed](#)]
15. Ou, E.; Xie, Y.; Peng, C.; Song, Y.; Peng, H.; Xiong, Y.; Xu, W. High concentration and stable few-layer graphene dispersions prepared by the exfoliation of graphite in different organic solvents. *RSC Adv.* **2013**, *3*, 9490–9499. [[CrossRef](#)]
16. Wang, B.; Liang, X. Surface Decoration and Dispersibility of Graphene Nanoplatelets in Aqueous Surfactant Solution. *J. Nanosci. Nanotechnol.* **2019**, *19*, 2060–2069. [[CrossRef](#)]
17. Vaghri, E.; Dorranean, D.; Ghoranneviss, M. Effects of CTAB concentration on the quality of graphene oxide nanosheets produced by green laser ablation. *Mater. Chem. Phys.* **2018**, *203*, 235–242. [[CrossRef](#)]
18. Du, W.; Jiang, X.; Zhu, L. From graphite to graphene: Direct liquid-phase exfoliation of graphite to produce single- and few-layered pristine graphene. *J. Mater. Chem. A* **2013**, *1*, 10592–10606. [[CrossRef](#)]
19. Wang, Z.; Chen, T.; Chen, W.; Chang, K.; Ma, L.; Huang, G.; Lee, J.Y. CTAB-assisted synthesis of single-layer MoS₂–graphene composites as anode materials of Li-ion batteries. *J. Mater. Chem. A* **2013**, *1*, 2202–2210. [[CrossRef](#)]
20. Yang, Y.J.; Li, W. CTAB functionalized graphene oxide/multiwalled carbon nanotube composite modified electrode for the simultaneous determination of ascorbic acid, dopamine, uric acid and nitrite. *Biosens. Bioelectron.* **2014**, *56*, 300–306. [[CrossRef](#)]
21. Zhong, C.; Wang, J.Z.; Wexler, D.; Liu, H.K. Microwave autoclave synthesized multi-layer graphene/single-walled carbon nanotube composites for free-standing lithium-ion battery anodes. *Carbon* **2014**, *66*, 637–645. [[CrossRef](#)]
22. Lotya, M.; King, P.J.; Khan, U.; De, S.; Coleman, J.N. High-concentration, surfactant-stabilized graphene dispersions. *ACS Nano* **2010**, *4*, 3155–3162. [[CrossRef](#)] [[PubMed](#)]
23. Ma, H.; Shen, Z.; Yi, M.; Ben, S.; Liang, S.; Liu, L.; Ma, S. Direct exfoliation of graphite in water with addition of ammonia solution. *J. Colloid Interface Sci.* **2017**, *503*, 68–75. [[CrossRef](#)] [[PubMed](#)]
24. Ren, L.; Qi, X.; Liu, Y.; Hao, G.; Huang, Z.; Zou, X.; Zhong, J. Large-scale production of ultrathin topological insulator bismuth telluride nanosheets by a hydrothermal intercalation and exfoliation route. *J. Mater. Chem.* **2012**, *22*, 4921–4926. [[CrossRef](#)]
25. Zhang, K.; Mao, L.; Zhang, L.L.; Chan, H.S.O.; Zhao, X.S.; Wu, J. Surfactant-intercalated, chemically reduced graphene oxide for high performance supercapacitor electrodes. *J. Mater. Chem.* **2011**, *21*, 7302–7307. [[CrossRef](#)]
26. Vadukumpully, S.; Paul, J.; Valiyaveetil, S. Cationic surfactant mediated exfoliation of graphite into graphene flakes. *Carbon* **2009**, *47*, 3288–3294. [[CrossRef](#)]
27. O'Neill, A.; Khan, U.; Nirmalraj, P.N.; Boland, J.; Coleman, J.N. Graphene dispersion and exfoliation in low boiling point solvents. *J. Phys. Chem. C* **2011**, *115*, 5422–5428. [[CrossRef](#)]
28. Sukumaran, S.S.; Tripathi, S.; Resmi, A.N.; Gopchandran, K.G.; Jinesh, K.B. Influence of surfactants on the electronic properties of liquid-phase exfoliated graphene. *Mater. Sci. Eng. B* **2019**, *240*, 62–68. [[CrossRef](#)]
29. Li, D.; Müller, M.B.; Gilje, S.; Kaner, R.B.; Wallace, G.G. Processable aqueous dispersions of graphene nanosheets. *Nat. Nanotechnol.* **2008**, *3*, 101. [[CrossRef](#)]
30. Ricardo, K.B.; Sendekci, A.; Liu, H. Surfactant-free exfoliation of graphite in aqueous solutions. *Chem. Commun.* **2014**, *50*, 2751–2754. [[CrossRef](#)]
31. Walch, N.J.; Nabok, A.; Davis, F.; Higson, S.P. Characterisation of thin films of graphene–surfactant composites produced through a novel semi-automated method. *Beilstein J. Nanotechnol.* **2016**, *7*, 209–219. [[CrossRef](#)] [[PubMed](#)]
32. Ferrari, A.C.; Meyer, J.C.; Scardaci, V.; Casiraghi, C.; Lazzeri, M.; Mauri, F.; Geim, A.K. Raman spectrum of graphene and graphene layers. *Phys. Rev. Lett.* **2006**, *97*, 187401. [[CrossRef](#)] [[PubMed](#)]
33. Hao, Y.; Wang, Y.; Wang, L.; Ni, Z.; Wang, Z.; Wang, R.; Thong, J.T. Probing layer number and stacking order of few-layer graphene by Raman spectroscopy. *Small* **2010**, *6*, 195–200. [[CrossRef](#)] [[PubMed](#)]

